

Strength function from the $^{113}\text{Cd}(n,\gamma)$ reaction

T. Belgya¹, L. Szentmiklósi¹, R. Massarczyk², R. Schwengner², G. Schramm², E. Birgersson², A. Junghans²

¹Nuclear Analysis and Radiography Department, Institute for Energy Security and Environmental Safety, Centre for Energy Research H-1525 POB 49, Budapest, Hungary

²Helmholtz-Zentrum Dresden-Rossendorf, Institute of Radiation Physics

Abstract

GENAT4 Monte Carlo simulations of the Budapest PGAA detector system are presented. The obtained response functions were used to unfold the spectrum from $^{113}\text{Cd}(n,\gamma)$ reaction – measured at the Budapest PGAA – in order to determine the γ -ray strength function. Preliminary results for the total radiative neutron capture cross sections for the $^{14}\text{N}(n,\gamma)$ and the $^{113}\text{Cd}(n,\gamma)$ reactions based on the unfolding approach are presented.

1 Introduction

Radiative capture of neutrons is a nuclear process of special importance for projects on the transmutation of radioactive waste. As capture channels compete with fission their knowledge is essential for the design of transmutation scenarios. For respective calculations performed on the basis of the Hauser-Feshbach formalism one needs the photon strength function governing the γ -decay to low lying final states from the capturing resonances in the continuum. As shown recently [1], photon scattering experiments performed at the ELBE facility have delivered data which can be described with a surprisingly successful parameterization of the electric dipole strength function in heavy nuclei using the so-called triple Lorentzian (TLO) strength function.

This triple Lorentzian concept [1] also describes various radiative neutron capture data hitherto interpreted in a different way [2]. Disagreeing predictions for photon strength functions have been in use by the two communities of neutron and photon beam experimenters – as documented in the IAEA reference input parameter library RIPL2 [2], where six different propositions based on capture data are listed for the calculation of E1-strengths. As also the microscopically calculated E1-strength function given there is at variance to many neutron capture as well as photon data [1] further investigations are urgently needed. In the recently started RIPL3-initiative [3] some of these deficiencies have been worked on, but the correlation between GDR width and nuclear triaxiality [1] is not properly accounted for.

One reason for the antagonism between the parameterizations resulting from photon respectively neutron capture data may be the fact that often different spins are populated making a direct comparison of data difficult. This difference can be minimized by using spin $\frac{1}{2}^-$ nuclei with A,Z for neutron capture to be compared to photo effect data in A+1,Z. Unfortunately, only very few pairs of stable isotopes A,Z and A+1,Z are available as targets for these comparative experiments.

A collaboration within the EU-EFNUDAT consortium, formed by the Centre for Energy Research (formerly Institute of Isotopes), Charles University and Helmholtz Zentrum Dresden-Rossendorf, has investigated first the $^{77}\text{Se}(n,\gamma)$ and the $^{78}\text{Se}(\gamma,\gamma')$ reactions. Both data sets have already been analysed and published [4]. The other favourable pair $^{195}\text{Pt}/^{196}\text{Pt}$ – belonging to a clearly different mass region – has also been evaluated and published [5]. It has been shown that

both the experimentally measured (n, γ) and (γ,γ') spectra can be described with a common strength function [4, 5].

In addition to the E1 strength the magnetic dipole (M1) strength also contribute to radiative capture. The study of complete gamma spectra following the capture of thermal neutrons in a spin $\frac{1}{2}^+$ -target may yield independent, interesting information for this case. It is thus proposed to extend the EFNUDAT-study for capture in spin $\frac{1}{2}^+$ -targets by also looking at the pair of $^{113}\text{Cd}(n,\gamma)$ and $^{114}\text{Cd}(\gamma,\gamma')$ reaction spectra. In this case the capture of thermal neutrons on ^{113}Cd was studied by the Compton suppressed HOGe-detector at the Budapest PGAA facility

To analyse the data the Budapest group had to improve the response function description of the PGAA detector. The group has already spent a substantial amount of efforts for calculating the response functions [6-8] with MCNP-CP and GEANT4. After making fine adjustment of the detector model in the GEANT4 Monte Carlo calculations, the response function simulation has reached a satisfactory degree of agreement between the calculations and experiments only recently and therefore we could use the current set of GEANT4 response function data modelled by GEANT4 for unfolding or stripping of experimental spectra. In this article we provide details on the PGAA response function modelling and about our methodology of unfolding, and some results, This work will facilitate the strength function determination of ^{114}Cd in collaboration with the Dresden group.

2 Experiments

The latest description of the Budapest PGAA facility has been published recently [9]. The experiments related to the detector response function utilized the PGAA sample chamber. This chamber can be evacuated to suppress the signals coming from the activation of the air in the sample chamber. Polymer sheets loaded with ^6Li -enriched LiF were used to cover the interior of the flight tube and the target chamber to shield against the neutrons scattered by the target. The gamma-rays emitted by the irradiated samples or by the calibration sources were measured with a 27% relative efficiency HPGe detector which is surrounded by a BGO guard annulus and heavy lead shielding. The gamma-ray spectra were accumulated in an acquisition computer with 16 K channel resolution, covering the 45 keV-12 MeV energy range.

The low energy detector response function were measured with a number of γ -ray standard sources, including ^{60}Co , ^{207}Bi , ^{133}Ba , ^{152}Eu . For higher energies, gamma-sources utilizing the neutron capture reactions of $\text{H}(n,\gamma)\text{D}$ and $^{14}\text{N}(n,\gamma)^{15}\text{N}$ in form of suitable H_2O and Urea-D targets were used.

The $^{113}\text{Cd}(n,\gamma)$ experiments were performed on enriched as well as on a high purity natural metal samples. The highly enriched sample was obtained from the USSR and its composition is given in Table 1.

Mass number								
106	108	110	111	112	113	114	115	Other elements
-	-	0.4	0.7	3.4	90.2	4.9	0.4	< 0.001

Table 1: Composition of the enriched ^{113}Cd sample in % of atom numbers

The natural sample was 50 μm thick, 99.99% pure cadmium metal sheet obtained from Goodfellow. The radiative neutron capture cross section of cadmium is so high that a pencil-beam with 1 mm^2 cross section could already provided sufficient to induce 1 k (suppressed) and 3 k (unsuppressed) counting rates. We measured both samples for about one day. The detector signal was split and acquired in both Compton-suppressed and unsuppressed modes. The dead time in the unsuppressed mode was 3.6% for the enriched sample and 3.2% for the natural sample. The visual comparison of the enriched and natural samples shows no significant difference between them. The dead time for the natural target measurements was 7.8% in the Compton-suppressed case and 7.2% for the enriched sample.

3 GEANT4 calculations for the response functions of the Budapest PGAA HPGe detector

The GEANT4 Monte Carlo simulation code[10] was used to generate the response functions of the Budapest PGAA detector. Several experimental conditions and X-ray radiographies for understanding the internal geometry of the detectors were used to study responses of HPGe detectors, including the Budapest PGAA detector [6], which were the starting point to build the more complex shielded geometry. The methodology of the calculation was to describe the measured response of our ^{60}Co point source as accurate as possible by making minor changes in the geometry obtained from the manufacturers and from the X-ray radiography of the HPGe detector. Drawings of the geometry are show in Figure 1.

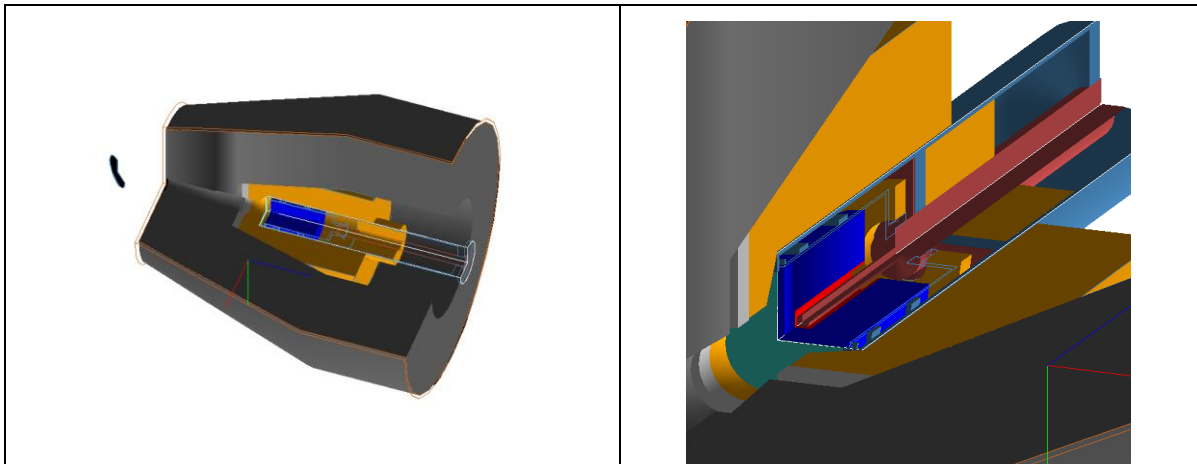


Figure 1: Drawing of the modelled detector geometries. Darker dray colour is the outer lead shielding, light gray is the main and catcher guard BGO detectors, and black is the Ge crystal. Many other details are not shown for the clarity.

The calculations were done in unsuppressed mode. We produced a list mode data file from the Monte Carlo code for the HPGe and BGO detectors to build up Compton suppression mode in separate replay calculations because the perfect anticoincidence did not provided satisfactory agreement with the experiment. The result of the Compton suppressed calculations will be presented in a separate paper. Here we concentrate only on results that can be obtained from the unsuppressed mode spectrum.

The calculated ^{60}Co spectrum was composed of the two gamma lines at 1173 keV and 1332 keV energies, by normalising them to the measured full energy peak areas. Figure 2 presents the agreement achieved for the ^{60}Co source measurement.

As it can be seen there is still some deviations below 400 keV, however this will not crucially influence the conclusions for higher energies. We achieved this quite satisfactory agreement after a long iteration procedure. At this point we decided to produce the response function as a function of the energy from 250 keV up to 12 MeV with a step of 250 keV with 1 keV binning. We call them as node spectra. The calculations took about 60 days of processor time on i5 Intel processors. All of our measured spectra were transformed to the 1 keV binning by a suitable algorithm to be able to compare them directly with the calculations.

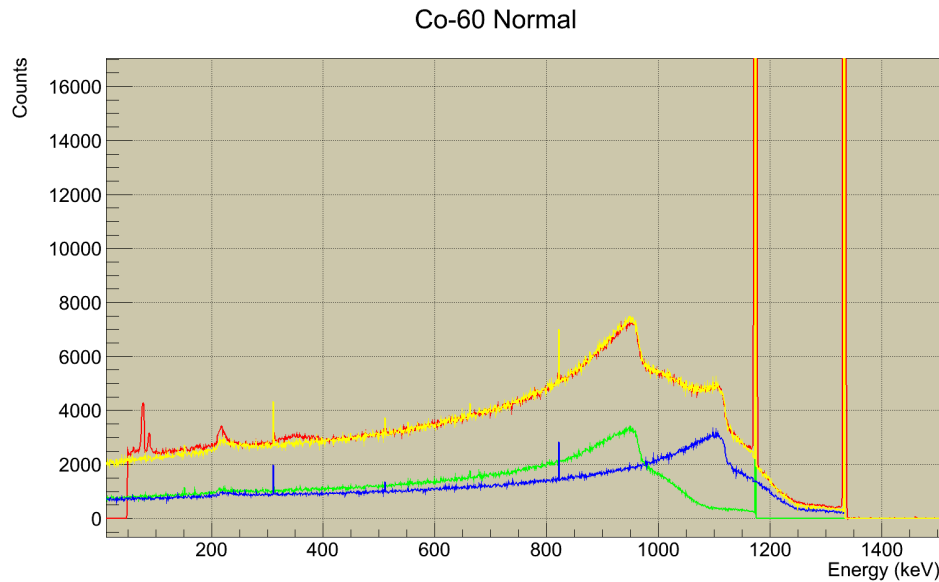


Figure 2. : The upper two curves are the simulated (black) and measured (grey) spectra of ^{60}Co calibration source. The two curves below are the simulated 1173 keV and 1332 keV full energy spectra; their weighted sum is the simulated curve.

We also decided to follow the treatment of the response functions according to the Oslo prescription [11]. We normalized all of the node spectra to one to form probability distributions. After the normalization, we removed the full energy, the single escape, the double escape and the Annihilation peaks. At the same time these event probabilities were fit with Cardinal-splines [12] for later use. Figure 3 shows the stripped node distributions that are suitable for interpolation.

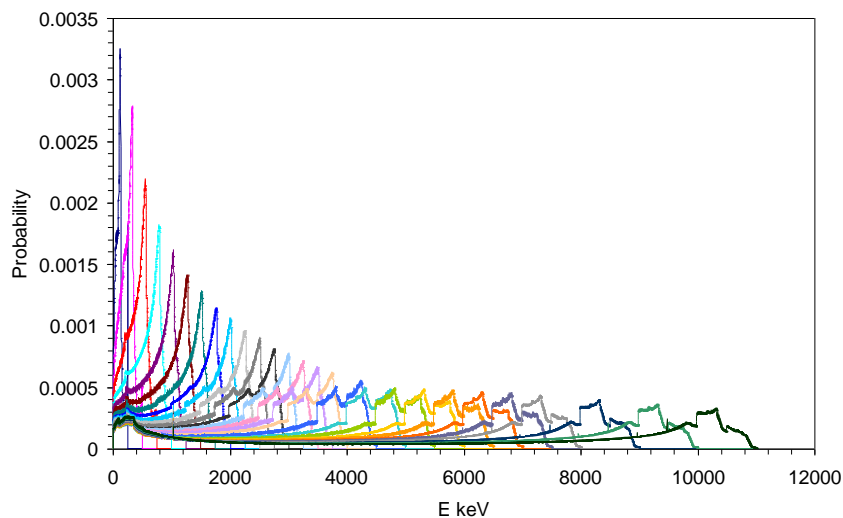


Figure 3.: The node response functions prepared for interpolation.

According to the Oslo prescription the interpolation for energy E of the Compton scattering part of the response function $c(E, E_\gamma)$ – belonging to the full energy peak of E_γ – can be done in the angle space θ using the two neighbouring node spectra between the Compton-edge and the backscattering peak.

$$c(E, E_\gamma) = \left(\frac{dE}{d\theta} \right)_{E_\gamma}^{-1} \left[c_1(E_1) \left(\frac{dE_1}{d\theta} \right)_{E_{\gamma 1}} + \frac{E_\gamma - E_{\gamma 1}}{E_{\gamma 2} - E_{\gamma 1}} \times \left(c_2(E_2) \left(\frac{dE_2}{d\theta} \right)_{E_{\gamma 2}} - c_1(E_1) \left(\frac{dE_1}{d\theta} \right)_{E_{\gamma 1}} \right) \right] \quad (1)$$

This is of course not true for the continuum belonging to the escape peaks; however we will neglect this here. Above the Compton-edge simple stretching and constriction interpolation is used similar to the one shown in Eq. (1). The quality of the interpolation is checked by direct comparison of the interpolated and simulated spectra. This is shown in Figure 4. As it can be seen in Figure 4 the interpolation is almost perfect with the Oslo method [11]. There seems to be a minor disagreement around the back scattered peak at about 220 keV for which the interpolation does not work well. This can also be treated by interpolating the back scattered peak as suggested but we neglected it since it does not contribute to our major goal of unfolding the ^{114}Cd spectrum significantly.

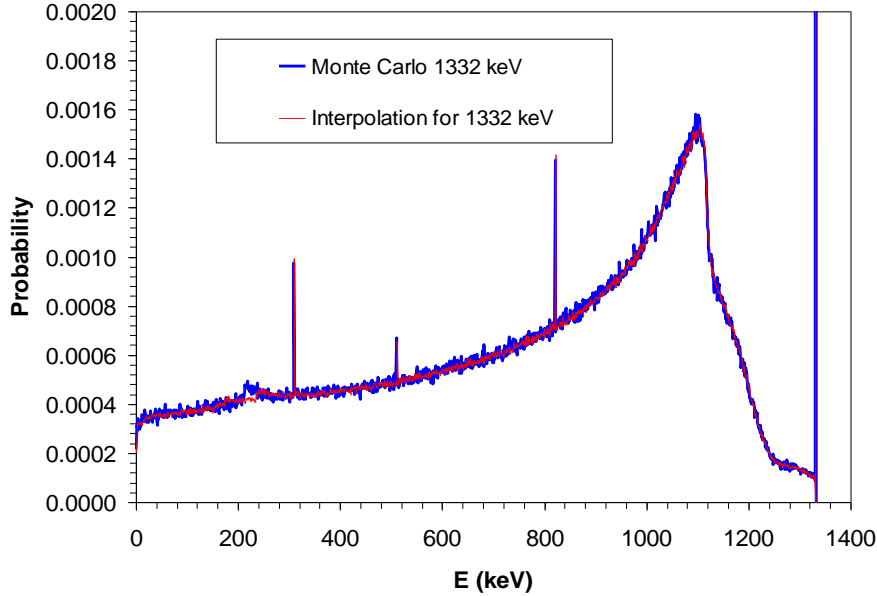


Figure 4: Comparison of the interpolated continuum and the GEANT4 Monte Carlo simulated spectra.

4 Unfolding of measured spectra, determination of capture cross sections

4.1 Unfolding procedure and results

Unfolding of spectra can be performed different ways. The simplest way is to start at the highest full energy peak that is detectable in the spectrum and consider its highest energy channel content

as a result of full energy deposition. Subtracting the corresponding full-energy point normalised response function from the whole spectrum will result in also a full energy point in the previous channel. This procedure can be repeated till the lowest channel for which response function was calculated. Of course any difference between the model and true response will accumulate bias in the process. In this study we neglect the calculation of the accumulated uncertainties and the effect of the peak width, which due to the small width do not influence the result much. In Figure 5 unfolding results for the ^{60}Co and ^{152}Eu calibration sources are shown.

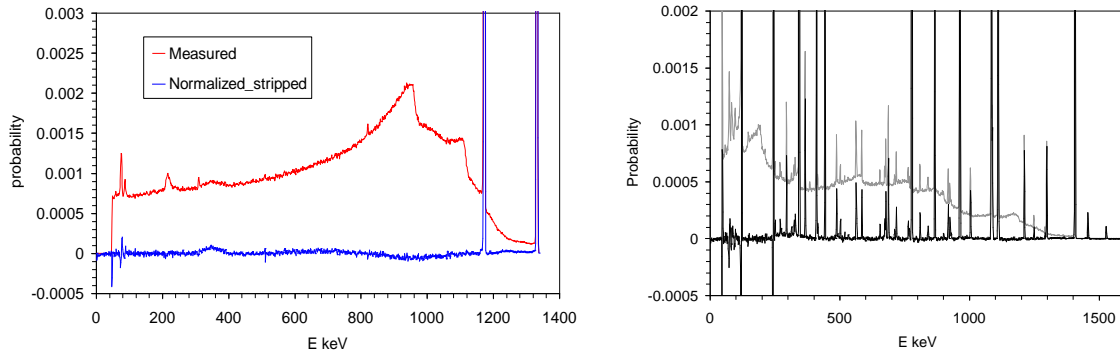


Figure 5: Unfolded ^{60}Co (left chart, black) and ^{152}Eu (right chart, black) calibration source spectra. The measured spectra (gray) were normalized to 1.

It can clearly be seen that the subtraction result in small differences where the continuum part of the response function is. The deviation from zero difference is smaller than 10% for most of the continuum and is positive and negative as well. The sum of differences is 0.0029 for the continuum and the summed peak area is 0.3618, the percentage of the continuum per peak area is 0.8%. For more complicated spectra it is more difficult to quantify.

Finally, we present the unfolding result for the $^{14}\text{N}(n,\gamma)$ and $^{113}\text{Cd}(n,\gamma)$ spectra in Figure 6.

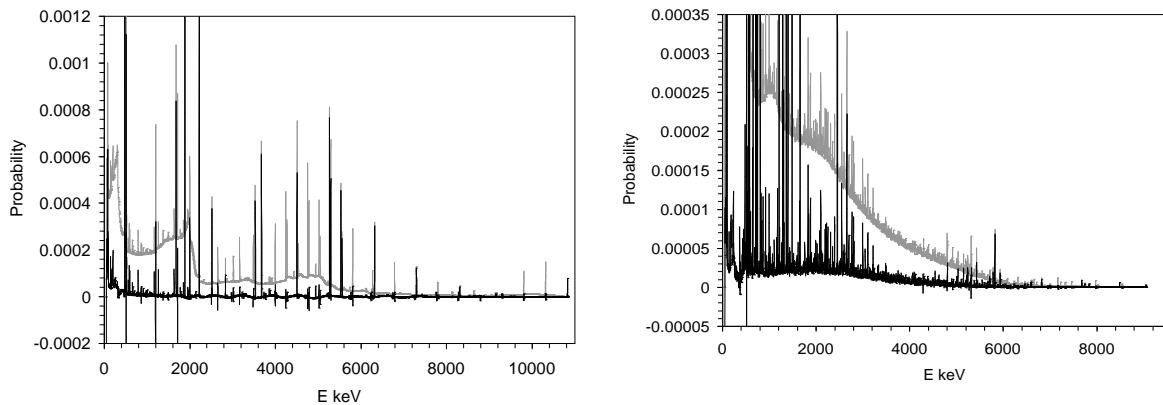


Figure 6: Unfolded $^{14}\text{N}(n,\gamma)$ (left chart, black) and $^{113}\text{Cd}(n,\gamma)$ (right chart, black) spectra. The measured spectra (gray) were normalized to 1.

It is clearly visible that the unfolding of relatively simple $^{14}\text{N}(n,\gamma)$ spectrum removed a large percentage of the continuum while the residuum has a periodic change between positive and negative values around zero. Peaks in the negative region are due to the difference of the full energy peak width and the escape peak width. The periodicity of the residuum can be correlated with the escape peak distances; however this statement has to be studied in detail. The unfolding of the far more complicated $^{113}\text{Cd}(n,\gamma)$ spectrum provides a significant bump with a centre of 2.2 MeV of positive values that can be associated with the expected quasi-continuum of full energy

peaks. It is important to note that the bump does not go to zero down to about 400 keV which means a large number of low energy transitions in the quasi-continuum.

4.2 Calculation of radiative capture cross sections

Before using the unfolded $^{14}\text{N}(n,\gamma)$ and $^{113}\text{Cd}(n,\gamma)$ spectra for total capture cross section calculation, they have to be corrected for full energy peak efficiency for which the measured and fitted efficiency curve was used. Since the unfolded spectra contain only full energy events they can be corrected with measured full energy efficiency for each channel. The efficiency-corrected unfolded $^{113}\text{Cd}(n,\gamma)$ spectrum and, the calculated and measured efficiency curves are shown in Figure 7.

Using the energy weighted sum rule [13] with internal calibration

$$\sigma_{\text{th}} = \sum_i \sigma_{\gamma i} E_i / B_n, \quad (2)$$

we can obtain the thermal capture cross section σ_{th} . In Eq. (2) $\sigma_{\gamma i}$ is the partial γ -ray production cross section for the i^{th} channel, E_i is its energy and B_n is the binding energy. In this formula there is no account for the possible conversion electron and internal pair-production [13] contributions.

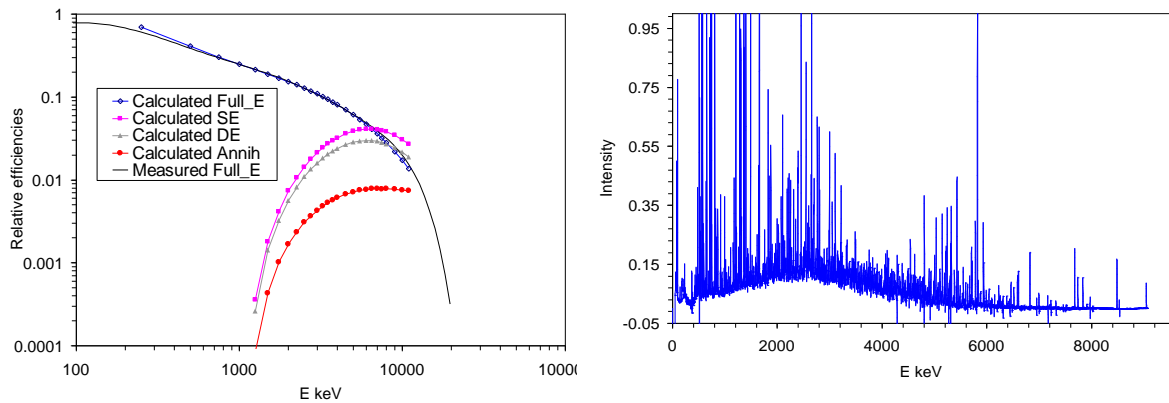


Figure 7: Measured and calculated relative efficiencies (left chart) and the full energy efficiency corrected $^{113}\text{Cd}(n,\gamma)$ spectrum (right chart).

For the $^{14}\text{N}(n,\gamma)$ thermal capture cross section Eq. (2) yields 90 mb, while the measured literature value is 80.3(8) mb [14]. This value contains the contribution from capture of ^{12}C from Urea-D, Cl and B impurities. The elimination of these impurity contributions requires more work. In the case of $^{113}\text{Cd}(n,\gamma)$ reaction the impurities can be neglected and the thermal capture cross section is 21640 b, while the literature value is 20600(400) b [15]. The agreement between the measured and literature values is quite good taking into the account that about 5-10% uncertainty can be assigned to the unfolding procedure. This agreement suggests that the procedure works rather well.

5 Conclusions

GENAT4 Monte Carlo simulations for the Budapest PGAA detector system were presented. It was shown that they can be adequately used to approximate measured spectra of various complexities.

The obtained response functions were used to unfold simple, as well as complicated spectra, including the measured $^{113}\text{Cd}(n,\gamma)$ spectrum which is our goal in the EFNUDAT and ERINDA collaborations. To check the quality of the procedure total thermal capture cross sections of the $^{14}\text{N}(n,\gamma)$ and $^{113}\text{Cd}(n,\gamma)$ reactions have been calculated and compared to the literature. The unfolded $^{113}\text{Cd}(n,\gamma)$ spectrum contains a broad bump of continuum centred around 2.2 MeV. It will be used to deduce the gamma ray strength function based on simulation of the decay scheme.

Acknowledgement

Support of EU FP6 EFNUDAT (EURATOM contract no. 036434), EU FP7 ERINDA (EURATOM contract no. 269499) and NKTH NAP VENEUS08 projects are acknowledged.

References

- [1] Junghans, A. R., G. Rusev, R. Schwengner, A. Wagner, and E. Grosse, *Phys. Lett. B* **670**(3) (2008) 200.
- [2] Belgia, T. et al., *Handbook for calculations of nuclear data, RIPL-2*, M. Herman, Editor. IAEA-TECDOC-1506: Vienna (2006)
- [3] Capote, R., M. Herman, P. Oblozinsky, P.C. Young, S. Goriely, T. Belgia, A.V. Ignatyuk, A.J. Koning, S. Hilaire, V.A. Plujko, M. Avrigeanu, O. Bersillon, M.B. Chadwick, T. Fukahori, Z.G. Ge, Y.L. Han, S. Kailas, J. Kopecky, V.M. Maslov, G. Reffo, M. Sin, E.S. Soukhovitskii, and P. Talou, *Nuclear Data Sheets*, **110**(12) (2009) 3107-3213.
- [4] Schramm, G., R. Massarczyk, A.R. Junghans, T. Belgia, R. Beyer, E. Birgersson, E. Grosse, M. Kempe, Z. Kis, K. Kosev, M. Krticka, A. Matic, K.D. Schilling, R. Schwengner, L. Szentmiklosi, A. Wagner, and J.L. Weil, *Phys. Rev. C* **85**(1) (2012) 014311 1-14.
- [5] Massarczyk, R., G. Schramm, A.R. Junghans, R. Schwengner, M. Anders, T. Belgia, R. Beyer, E. Birgersson, A. Ferrari, E. Grosse, R. Hannaske, Z. Kis, T. Kögler, K. Kosev, M. Marta, L. Szentmiklósi, A. Wagner, and J.L. Weil, *Phys. Rev. C* **87** (2013) 044306.
- [6] Szentmiklosi, L., T. Belgia, B. Maroti, and Z. Kis, *J. Nucl. Radioanal. Chem.* (2014) submitted.
- [7] Szentmiklosi, L., Z. Kis, T. Belgia, and A.N. Berlizov, *J. Radioanal. Nucl. Chem.* **298** (2013) 1605.
- [8] Szentmiklósi, L., Berlizov, A.N., *Nucl. Instr. Meth. A* **612** (2009) 122-126.
- [9] Szentmiklósi, L., T. Belgia, Z. Révay, and Z. Kis, *J. Radioanal. Nucl. Chem.* **286** (2010) 501-505.
- [10] Agostinelli, S.e.a., *Nucl. Instrum. Methods Phys. Res. A* **506** (2003) 250.
- [11] Guttormsen, M., T.S. Tveter, L. Bergholt, F. Ingebretsen, and J. Rekstad, *Nucl. Instr. Meth. A* **374** (1996) 371.
- [12] Belgia, T., *J. Nucl. Radioanal. Chem.* **265**(2) (2005) 175-179.
- [13] Belgia, T., *J. Nucl. Radioanal. Chem.* **276**(3) (2008) 609-614.
- [14] Belgia, T., *Phys. Rev. C* **74** (2006) 024603-1-8.
- [15] Mughabghab, S.F., IAEA INDC(NDS)-440 (2003).